

This discussion paper is/has been under review for the journal Atmospheric Chemistry and Physics (ACP). Please refer to the corresponding final paper in ACP if available.

**Patterns of mercury
dispersion from
emission sources**

A. Kolker et al.

Patterns of mercury dispersion from local and regional emission sources, rural Central Wisconsin, USA

A. Kolker¹, M. L. Olson², D. P. Krabbenhoft², M. T. Tate², and M. A. Engle¹

¹US Geological Survey, Eastern Energy Resources Science Center, Reston, VA, 20192, USA

²US Geological Survey, Wisconsin Water Science Center, Middleton, WI, 53562, USA

Received: 16 December 2009 – Accepted: 18 December 2009 – Published: 21 January 2010

Correspondence to: A. Kolker (akolker@usgs.gov)

Published by Copernicus Publications on behalf of the European Geosciences Union.

Title Page

Abstract

Introduction

Conclusions

References

Tables

Figures

◀

▶

◀

▶

Back

Close

Full Screen / Esc

Printer-friendly Version

Interactive Discussion



Abstract

Simultaneous real-time changes in mercury (Hg) speciation – reactive gaseous Hg (RGM), elemental Hg (Hg°), and fine particulate Hg ($\text{Hg-PM}_{2.5}$), were determined from June to November 2007, in ambient air at three locations in rural Central Wisconsin.

Known Hg emission sources within the airshed of the monitoring sites include: 1) a 1114 megawatt (MW) coal-fired electric utility generating station; 2) a Hg-bed chlor-alkali plant; and 3) a smaller (465 MW) coal-burning electric utility. Monitoring sites, showing sporadic elevation of RGM, Hg° and $\text{Hg-PM}_{2.5}$, were positioned at distances of 25, 50 and 100 km northward of the larger electric utility. A series of RGM events were recorded at each site. The largest, on 23 September, occurred under prevailing southerly winds, with a maximum RGM value (56.8 pg m^{-3}) measured at the 100 km site, and corresponding elevated SO_2 (10.41 ppbv; measured at 50 km site). The finding that RGM, Hg° , and $\text{Hg-PM}_{2.5}$ are not always highest at the 25 km site, closest to the large generating station, contradicts the idea that RGM decreases with distance from a large point source. This may be explained if: 1) the 100 km site was influenced by emissions from the chlor-alkali facility or by RGM from regional urban sources; 2) the emission stack height of the larger power plant promoted plume transport at an elevation where the Hg is carried over the closest site; or 3) RGM was being generated in the plume through oxidation of Hg° . Operational changes at each emitter since 2007 should reduce their Hg output, potentially allowing quantification of the environmental benefit in future studies.

1 Introduction

Atmospheric emissions, transport and deposition of mercury (Hg) are key processes leading to the global mercury contamination problem (Wiener et al., 2003). Mercury emissions to the atmosphere arise from natural and anthropogenic sources, and by re-emission of previously deposited Hg (reviewed by Banic et al., 2005). Speciation

Patterns of mercury dispersion from emission sources

A. Kolker et al.

Title Page

Abstract

Introduction

Conclusions

References

Tables

Figures

◀

▶

◀

▶

Back

Close

Full Screen / Esc

Printer-friendly Version

Interactive Discussion



of atmospheric mercury is influenced by a combination of local emission sources, generally contributing a greater proportion of reactive species, and global long range transport of long lived species such as Hg°. Among local sources, the location, type of emitter, and amount of Hg emitted may be characteristic in distinguishing their contribution to the mercury budget of a given area.

In the present study, we set up three receptor stations at different locations within a rural study area having no major anthropogenic Hg emission sources within 25 km or more. Using this three-receptor array, changes in mercury speciation were continuously monitored, ultimately showing the influence of three Hg emission sources located at the periphery of the study area in opposing directions (Fig. 1), as well as regional sources from major urban areas of the US Midwest. The goals of the study were to: 1) distinguish multiple Hg inputs in a rural setting with relatively few Hg sources, that are directionally distinct; 2) track possible conversion between atmospheric Hg species; and 3) test the efficacy of simultaneous deployment of mercury speciation monitoring stations for possible use by the National Atmospheric Deposition Program (NADP) Atmospheric Mercury Network (AMNet).

2.1 Study area

The study area is predominantly agricultural with no major topographic barriers or resulting orographic effects between the sampling sites. The sampling sites are positioned at the easternmost margin of the Central Wisconsin Sand Plains physiographic province, an area of low relief comprising the basin of Glacial Lake Wisconsin, or in adjacent low-relief outwash areas to the east (e.g., Hooyer, 2001). From the 50 km site, Hg emission sources closest to the study area are located to the south, to the northwest, and to the north-northwest, potentially making it possible to delineate their input on the basis of local wind patterns. The orientation of the sampling array was coincident with winds from the south, the most prevalent wind direction occurring during the summer and early fall in this part of Wisconsin, based on analysis of historic wind records. Field investigation spanned the period from June to November 2007.

Patterns of mercury dispersion from emission sources

A. Kolker et al.

Title Page

Abstract

Introduction

Conclusions

References

Tables

Figures

◀

▶

◀

▶

Back

Close

Full Screen / Esc

Printer-friendly Version

Interactive Discussion



Patterns of mercury dispersion from emission sourcesA. Kolker et al.

[Title Page](#)[Abstract](#)[Introduction](#)[Conclusions](#)[References](#)[Tables](#)[Figures](#)[⏪](#)[⏩](#)[◀](#)[▶](#)[Back](#)[Close](#)[Full Screen / Esc](#)[Printer-friendly Version](#)[Interactive Discussion](#)

To track possible changes in mercury speciation associated with conversion between atmospheric Hg species during transport, Tekran speciation units were deployed at sampling sites with distances of 25, 50, and 100 km along a line northward starting at one of the mercury sources, a combined 1114 MW utility generating station burning Powder River Basin (PRB) coal. PRB coal is characteristically low in sulfur, and in mercury, with a mean Hg content of 0.08 ppm for 612 samples in the USGS COALQUAL database (Bragg et al., 1998; Tewalt et al., 2001).

Following completion of field measurements in 2007, significant operational changes were made to the three mercury emission sources adjoining the study area. In 2008, a new 525 MW generating unit burning PRB coal was added to the 465 MW multi-unit coal-fired electric utility located about 50 km NNW of the 100 km site (Peltier, 2008). Modifications to the existing 465 MW capacity are also underway to upgrade its emission controls (Electric Energy Online, 2009). The new 525 MW unit is equipped with an activated carbon injection system to control mercury emissions and state-of-the-art controls for NO_x, SO₂, and particulate emissions (Campbell et al., 2009). At the chlor-alkali plant located about 35 km WSW of the 100 km site, conversion to mercury-free membrane technology is underway as part of an expansion of this facility (Hawthorne, 2007). Finally, at the 1114 MW utility at the southernmost end of the study area, equipment and operational modifications to reduce emissions of NO_x, SO₂ and Hg have been put in place or are planned. These changes make it impossible to replicate the local source conditions observed during the study, but source conditions similar to those sampled existed in the study area for an extended period up to and including 2007. With these changes, the contribution of local sources to transient atmospheric mercury levels in the study area should be reduced and future studies should allow for quantification of their environmental benefit.

2.2 Sampling methods

The USGS Mobile Atmospheric Mercury Laboratory (Mobile Lab; Kolker et al., 2007) was deployed at the 50 km site from June to November 2007. The Mobile Lab utilizes

Patterns of mercury dispersion from emission sourcesA. Kolker et al.

[Title Page](#)[Abstract](#)[Introduction](#)[Conclusions](#)[References](#)[Tables](#)[Figures](#)[◀](#)[▶](#)[◀](#)[▶](#)[Back](#)[Close](#)[Full Screen / Esc](#)[Printer-friendly Version](#)[Interactive Discussion](#)

a Tekran 1130/1135 mercury speciation unit coupled to a Tekran 2537A (serial #219) cold vapor atomic fluorescence spectrometer (CVAFS; hereafter, “speciation system” for both Tekran instruments combined). The Mobile Lab speciation system was one of three fixed speciation systems deployed concurrently. Other fixed Tekran speciation systems were deployed at the 25 km site (#236) and the 100 km site (#173). A 4th speciation system (#153) was alternated, first deployed in tandem with the Mobile Lab at the 50 km site (8 August–25 September), then moved to the 100 km site (27 September–22 November) for replicate measurements. In addition to its mercury speciation capability, the Mobile Lab has sampling and measurement capabilities for NO_x, SO₂, ozone, PM_{2.5} mass, and meteorological parameters that can be used in conjunction with mercury speciation results. Portable meteorological stations were deployed at the 25 km and 100 km sites.

In addition to continuous monitoring of mercury speciation over a 6-month period, more intensive sampling of particulate matter (PM) was conducted over a 10-d period in July/August, 2007. During this period, low volume USGS-design PM_{2.5} (16.7 L min⁻¹) or total suspended particulate (TSP; ~30 L min⁻¹) samplers (Kolker et al., 2008) were deployed at each of the three mercury speciation sites (25, 50, and 100 km). Additionally, at the 50 km site a commercial-design high volume (1500 L min⁻¹) TSP sampler (Tisch Environmental TE-5000) was used concurrently with the low volume sampler for the same period. Using the low volume samplers, total particulate Hg (Hg-TSP), or Hg-PM_{2.5}, were collected on pre-fired 47 mm quartz fiber filters. Using the high volume TSP, aerosols were collected on pre-fired 20×25 cm quartz fiber filters. For each dedicated PM sampler, the sampling orifice was mounted at a height of 2 m.

2.3 Analysis methods

Atmospheric Hg speciation systems deployed within the Mobile Lab and at the other two sampling sites (25 km and 100 km) utilize a Tekran 1130/1135 speciation unit coupled to a Tekran 2537A CVAFS. The system has been described elsewhere in greater

detail (e.g., Landis et al., 2002; Engle et al., 2008; Kolker et al., 2008; and references therein). To determine Hg speciation, RGM is sequentially collected on a KCl-coated annular denuder, fine particulate Hg-PM_{2.5} is collected on a re-generable particulate filter and Hg⁰ is collected on gold traps. The three mercury species collected are thermally desorbed and analyzed by the Tekran 2537A as Hg⁰. Every 2 h the atmospheric Hg speciation system provides 12 consecutive 5-min average Hg⁰ concentrations and 1-h integrated Hg-PM_{2.5} and RGM concentrations. The instruments were calibrated daily by an internal Hg⁰ permeation source. The Hg⁰ permeation sources were certified monthly. Pre-spiked denuders containing 48.4 pg RGM (Frontier Geosciences) were analyzed by the speciation units to demonstrate both the accuracy and precision of the instruments (recovery=98.6±13.1%, n=28). To determine the variability of the four speciation systems used in this study, tests were conducted whereby the units were attached to a single high-volume unheated manifold and exposed to ambient air, Hg⁰-spiked ambient air, and RGM-spiked ambient air. Runs were made on the manifold system between April 2007 and November 2008, totaling more than 19 d of operation. Results from the April 2007 manifold study, conducted prior to the measurement period for this study, showed that the average percent relative standard deviation (%RSD) between the four instruments was 5.9% for Hg⁰ (mean concentration=10.9 ng m⁻³), 34.2% for RGM (mean concentration=2.6 pg m⁻³), and 8.3% for Hg-PM_{2.5} (mean concentration=5.8 pg m⁻³). Testing during November 2008, demonstrated that %RSD values for RGM and Hg-PM_{2.5} decreased dramatically during exposure to higher concentrations. For example, %RSD for RGM concentrations <10 pg m⁻³ was 14.2% but improved to 9.8% at >10 pg m⁻³.

Exposed quartz fiber filters and filter blanks were analyzed by CVAFS according to methods modified from Olund et al. (2004) for particulate mercury in water samples. Filters are digested in PTFE bombs in a 5% BrCl solution, at 50°C for 5 d, to insure complete oxidation of particle-bound Hg to soluble forms. Sample digestion and analysis were carried out at the USGS Wisconsin Water Science Center Mercury Laboratory, in Middleton, Wisconsin, using an automated flow injection system in which a CVAFS

Patterns of mercury dispersion from emission sources

A. Kolker et al.

Title Page

Abstract

Introduction

Conclusions

References

Tables

Figures

◀

▶

◀

▶

Back

Close

Full Screen / Esc

Printer-friendly Version

Interactive Discussion



system is incorporated (Olund et al., 2004). A detection limit of 18 pg was attained for filter extracts based on analysis of 7 field blanks, corresponding to $\sim 0.71 \text{ pg m}^{-3}$ for $\text{Hg-PM}_{2.5}$ in air.

3 Results and discussion

3.1 Mercury speciation

Near continuous monitors of mercury speciation were obtained at the 25, 50, and 100 km sites from June through November of 2007. Summary results for RGM, Hg° and $\text{Hg-PM}_{2.5}$ are shown in Fig. 2. Baseline RGM levels are generally less than 3 pg m^{-3} , with short term excursions approaching or exceeding 30 pg m^{-3} (e.g., on 23 September). For Hg° , baseline concentrations are less than 2 ng m^{-3} with excursions approaching or exceeding 5 ng m^{-3} (e.g., on 12 November).

Results given in Fig. 2 include unqualified speciation data, shown as solid lines, and speciation results that have been flagged for one or more quality assurance (QA) concerns, shown as lighter-colored equivalents. QA flags include an incomplete sampling cycle (less than 1 h of sampling), Hg° measurements taken during the hour that manual Hg° injection occurred, baseline voltage or baseline deviation problems, etc. Results are omitted for first two Hg° measurements of the Hg° cycle, during Hg° manual air injections, and in all other cases where Hg° data are questionable or the speciation system is not functioning properly. Where speciation system unit #153 is used to duplicate the output of fixed unit #219 at the 50 km site (8 August–25 September) and #173 at the 100 km site (27 September–22 November) the replicates show good agreement (Fig. 2).

The large RGM peak detected at each site on 23 September is reflected in a much lesser increase in Hg° ; SO_2 and NO_x concentrations measured at the 50 km site were also elevated. Transient, correlated RGM- SO_2 peaks at near-baseline Hg° or $\text{Hg-PM}_{2.5}$ are noted by Manolopoulos et al., (2007; Devil's Lake, Wisconsin, USA) and

Patterns of mercury dispersion from emission sources

A. Kolker et al.

Title Page

Abstract

Introduction

Conclusions

References

Tables

Figures

◀

▶

◀

▶

Back

Close

Full Screen / Esc

Printer-friendly Version

Interactive Discussion



Patterns of mercury dispersion from emission sources

A. Kolker et al.

Title Page

Abstract

Introduction

Conclusions

References

Tables

Figures

◀

▶

◀

▶

Back

Close

Full Screen / Esc

Printer-friendly Version

Interactive Discussion



Kolker et al., (2008; Shenandoah National Park, Virginia, USA), for study areas that are largely rural and lack anthropogenic emission sources. This combination is characteristic of plumes from coal-fired generating stations (e.g., Edgerton et al., 2006). On 23 September, all three sites were downwind of the 1114 MW utility. However, during the 23 September RGM event, a larger RGM peak (56.8 pg m^{-3}) was found at the 100 km site than at the 25 km site (36.2 pg m^{-3}) or a qualified peak at the 50 km site (28.1 pg m^{-3} ; Fig. 3). Corresponding Hg° is also somewhat elevated at the 100 km site (1.755 ng m^{-3}) relative to the 25 and 50 km sites (1.532 and 1.558 ng m^{-3} , respectively). Although ground-level winds on 23 September reflect transport from the south, the data series shows that first arrival and peak response for RGM on this date occurred at the 100 km site. At the other two sites, closer to the inferred source, arrival times for peak RGM were approximately coincident, with corresponding peak RGM and SO_2 at the 50 km site (Table 1). In addition, the ratio of $\text{RGM}/\text{Hg}^{\circ}$, which would be expected to decrease with transport and conversion of RGM to Hg° from a single source, shows a reverse trend on 23 September, with a lower value at the 25 km site (0.015 expressed as a weighted ratio for the entire event) than at the 100 km site (0.020).

A pattern similar to that of 23 September is seen on 3 and 4 October, where peak RGM values at the 100 km site (9.9 and 15.2 pg m^{-3} , respectively) exceed smaller ($\leq 5 \text{ pg m}^{-3}$) corresponding peaks at the 25 and 50 km sites, under southerly wind conditions. In at least one other case (20 October) peak RGM does show a regular concentration decrease from the 25 km site (15.20 pg m^{-3}) to the 50 km site (13.15 pg m^{-3}) to the 100 km site (8.20 pg m^{-3}), and a corresponding decrease in event-weighted $\text{RGM}/\text{Hg}^{\circ}$, from 0.005 to 0.004, where the 100 km site is the farthest downwind. The finding that RGM is not always highest at the 25 km site, closest the 1114 MW utility, could be explained if: 1) another RGM source, such as the chlor-alkali plant, or more distal regional sources, contributed to Hg speciation at the 100 km site; 2) Hg from the 1114 MW utility is carried over the 25 km site at a high altitude as a result of its stack design parameters; or 3) RGM was being generated within the plume through oxidation of Hg° . Because the mercury cell chlor-alkali plant is a such a large emitter, it

may be a significant RGM source, even though this process generates predominantly Hg⁰ (Southworth et al., 2004; Landis et al., 2004) with small fractions of RGM present (Landis et al., 2004).

Hg-PM_{2.5} baseline values are generally less than 10 pg m⁻³ (Fig. 2) with more frequent excursions ≥ 20 –25 pg m⁻³, and some values in excess of 100 pg m⁻³ (on 20 June, 24 July, and 16 August). For the period of intensive PM_{2.5} sampling, time-averaged Hg-PM_{2.5} concentrations (by automated speciation system) for the three sampling sites are similar, with median values ranging from 10.8–11.8 pg m⁻³ (see the following section).

3.2 Intensive Hg-PM_{2.5} sampling

Intensive PM sampling occurred from 25 July to 5 August 2007, and included manual Hg-TSP at all three sites and manual Hg-PM_{2.5} at the 25 and 50 km sites, determined at 12-h intervals, in addition to the continued Hg-PM_{2.5} output of the speciation systems at each site (Fig. 4). A washout event that occurred on 27 July 2007 is seen as an Hg-TSP or Hg-PM_{2.5} minimum at all sites. Comparison of the manual Hg-TSP with the summed 12-h speciation system Hg-PM_{2.5} output intervals shows that in virtually all cases, the manual Hg-TSP equals or is greater than the automated Hg-PM_{2.5} output, showing that coarse particulate Hg may be present and is missed by the automated analyzers as a result of their 2.5 μ m input limitation (Fig. 4). Similar results have been found in previous direct comparisons between these approaches, especially where a large fraction of particulate Hg resides in the \geq PM_{2.5} fraction (Engle et al., 2008).

Where manually determined 12-h Hg-PM_{2.5} concentrations were compared with summed 12-h speciation system Hg-PM_{2.5} (at 25 km site and 50 km sites) the results show no statistically significant difference in the two approaches (Fig. 5), with a regression comparison biased slightly to the manual approach, giving a slope of 0.84 and an r^2 of 0.55. Consistency between the manual and automated approaches for Hg-PM_{2.5} indicates that comparison between Hg-TSP and speciation system Hg-PM_{2.5}

Patterns of mercury dispersion from emission sources

A. Kolker et al.

Title Page

Abstract

Introduction

Conclusions

References

Tables

Figures

◀

▶

◀

▶

Back

Close

Full Screen / Esc

Printer-friendly Version

Interactive Discussion



discussed above is valid because the filter-based approach used has not been subject to artifacts resulting from adherence or loss of gaseous mercury to or from the filter media (e.g., Malcolm and Keeler, 2007).

3.3 Directional mercury and ancillary gas concentration data

5 Directional patterns of mercury and ancillary gas distribution for the period from June to November 2007 are shown by concentration roses for RGM, Hg° , and $\text{Hg-PM}_{2.5}$ for each site, and SO_2 and NO_x roses for the 50 km site (Fig. 6). For RGM, the highest events recorded ($\geq 30 \text{ pg m}^{-3}$) are at the 100 km site, with the prevailing wind from the south, the direction of the 1114 MW power station. At this site, lesser RGM highs are
10 seen with winds from the WSW, the direction of the chlor-alkali plant, from the NNW, the direction of the 465 MW coal burning utility, and from the SE, in the direction of more distal power plant sources in the urbanized corridor along the shores of Lake Michigan, near the Illinois/Wisconsin border. At the 25 km site, RGM highs occur with southeast winds, towards these regional emission sources, in addition to highs occurring under
15 due-south winds, towards the 1114 MW power station. The due-south RGM highs at the 25 km site are less pronounced than at the 100 km site, even though the 25 km site is closer to this emitter.

For Hg° , the most pronounced directional highs ($\geq 3 \text{ ng m}^{-3}$) are at the 50 km site, when winds are from the northwest, towards the chlor-alkali plant. For $\text{Hg-PM}_{2.5}$, highs
20 ($\geq 20 \text{ pg m}^{-3}$) occur at the 25 km site with winds from the south, towards the 1114 MW power station; at the 50 km site with winds from the NW, towards the chlor-alkali plant; and at the 100 km site with winds from the WSW, also the direction of the chlor-alkali plant (Fig. 6). Similar rose-diagram treatment of SO_2 and NO_x data for the 50 km site shows considerable scatter, with the most pronounced directional trend being towards
25 the south (1114 MW utility) for each ancillary gas. For the pronounced Hg° high at the 50 km site with winds from the northwest, the lack of a corresponding SO_2 high is consistent with influence by the chlor-alkali plant, as suggested above.

Patterns of mercury dispersion from emission sources

A. Kolker et al.

Title Page

Abstract

Introduction

Conclusions

References

Tables

Figures

◀

▶

◀

▶

Back

Close

Full Screen / Esc

Printer-friendly Version

Interactive Discussion



Comparison of cumulative RGM results for the three sites as a function of wind direction is shown in Fig. 7. When winds are from the south (170–190°; Fig. 7a), of the three sites, the 100 km site consistently shows the highest RGM values, whereas RGM values for the other two sites are indistinguishable. When winds are from all other directions (190–170°; Fig. 7b), RGM values for all three sites are indistinguishable. This finding is counter to conventional thinking and assumptions applied to Hg transport modeling suggesting a mercury dispersion “halo” exists around large emission sources, whereby RGM is expected to decrease with distance from a central high as a function of dispersion and conversion to Hg° (Bullock et al., 1998; Cohen et al., 2004; Lee and Keener, 2008).

3.4 Air-mass back trajectories

Mercury speciation data, ancillary gas data, and directional information discussed above show that local emission sources at the periphery of the study area result in periodic elevation of RGM, Hg° and, for transient plumes from coal-burning utilities, correlated RGM and SO₂. The contribution of regional sources is more difficult to assess without knowing the back-trajectory of air-masses being sampled in the study area. Using the NOAA HYSPLIT model (Draxler and Rolph, 2003), backward air mass trajectories were simulated for the 23 September, 4 October, and 20 October 2007 events, in which RGM peaks occurred under the influence of southern winds. Results show significant variation in source areas depending on the ending height of the trajectory (i.e., 10 m, 500 m, 1000 m; Fig. 8). Given that all peaks investigated occurred during daytime, significant mixing was likely occurring in the boundary layer and variations in contributions from the various source areas likely occurred between the three sampling sites. For example, trajectories corresponding to the RGM pulse on 23 September 2007 ending at heights of 100 and 500 m, originated near Chicago, a significant regional source area for atmospheric Hg, and were modeled to have been transported near the coal-fired utility power station due south of the receptor sites (Fig. 8).

Patterns of mercury dispersion from emission sources

A. Kolker et al.

Title Page

Abstract

Introduction

Conclusions

References

Tables

Figures

◀

▶

◀

▶

Back

Close

Full Screen / Esc

Printer-friendly Version

Interactive Discussion



These findings suggest that contributions from multiple sources may have been responsible for elevated RGM concentration during this and other events, and this may help explain the unexpected first arrival of the source plume at the furthest monitoring site.

4 Conclusions

Three simultaneously operated atmospheric mercury sites in rural Central Wisconsin show sporadic elevation of RGM, Hg^0 and $\text{Hg-PM}_{2.5}$. Correspondence of elevated Hg species varies between sites; correspondence between elevated mercury species and ancillary gas levels is similarly variable. These variations are likely the result of differing contributions of local-to-regional scale emission sources and variation in air mass transport direction. Some RGM peaks have associated SO_2 peaks, together indicative of plumes from coal burning utility power stations, whereas others do not, indicating they are more likely derived from the mercury-bed chlor-alkali facility. The greatest peak response concentrations were commonly observed at the 100 km site, farthest from the largest power plant Hg emission source. This suggests that the 100 km site is most-likely impacted by other Hg sources, in addition to the 1114 MW power station to the south. Overall, highest RGM concentrations occur with air masses from the south (all sites) or the northwest (25, 50 km sites), or west-southwest (100 km site), downwind of the two largest mercury sources. Short-term manual replication of $\text{Hg-PM}_{2.5}$ shows good agreement with automated $\text{Hg-PM}_{2.5}$ measurements, thereby validating the filter-based collection method. Manual Hg-TSP determination indicates that significant fractions of particulate mercury may be coarser than the $2.5\mu\text{m}$ orifice limitation of the automated speciation systems. HYSPLIT air mass back-trajectories are helpful in assessing the contribution of mercury from regional sources such as major cities, and in showing divergence in transport at differing levels of the atmosphere. This approach is not useful in distinguishing among the local sources at the periphery of the study area, because the back-trajectory grid-size (40 km) is too coarsely

Patterns of mercury dispersion from emission sources

A. Kolker et al.

Title Page

Abstract

Introduction

Conclusions

References

Tables

Figures

◀

▶

◀

▶

Back

Close

Full Screen / Esc

Printer-friendly Version

Interactive Discussion



spaced. Operational changes to the local emission sources make it impossible to replicate conditions of the study, but these changes have the overall effect of reducing mercury emissions in the study area.

Acknowledgements. This study was supported by an interagency agreement (#DW-14-922332-01) between the USGS and the US EPA Office of Air and Radiation, Clean Air Markets Division. Field work by Engle and Kolker was supported by the US Geological Survey Toxic Substances Hydrology (Toxics) Program, and the USGS Energy Resources Program. We acknowledge support of the USGS Toxics Program for participation (by Kolker) in the 9th International Conference on Mercury as a Global Pollutant, where an earlier version of this paper was presented. We thank Casey Soneira and John DeWild for assistance in the field and Nicholas Geboy for help in preparation of figures. Use of trade, product, or firm names is for descriptive purposes only and does not imply endorsement by the US Government.

References

- Banic, C., Blanchard, P., Dastoor, A., Hung, H., Steffen, A., Tordon, R., Poissant, L., and Wiens, B.: Atmospheric distribution and long-range mercury transport, in: Mercury: Sources, measurements, cycles, and effects, edited by: Parsons, M. B. and Percival, J. B., Mineralogical Association of Canada, Short Course Series, 34, 157–177, 2005.
- Bragg, L. J., Oman, J. K., Tewalt, S. J., Oman, C. L., Rega, N. H., Washington, P. M., and Finkelman, R. B.: US Geological Survey Coal Quality (COALQUAL) Database: Version 2.0: US Geological Survey Open File Report 97-134, CD-ROM, 1998.
- Bullock, O. R., Brehme, K. A., and Mapp, G. R.: Lagrangian modeling of mercury air emission, transport and deposition: an analysis of model sensitivity to emissions uncertainty, *Sci. Total Environ.*, 213(1–3), 1–12, 1998.
- Campbell, T., Gertz, F. X., Mataczynski, K., Amrhein, G. T., Filippelli, G., and Stewart, R.: Mercury control optimization study at Wisconsin Public Service Weston Unit 4, in: Proceedings, Air Quality VII, Arlington, VA, Oct, 2009, 12, 2009.
- Cohen, M., Artz, R., Draxler, R., Miller, P., Poissant, L., Niemi, D., Ratté, D., Deslauriers, M., Duval, R., Laurin, R., Slotnick, J., Nettesheim, T., and McDonald, J. L.: Modeling the atmospheric transport and deposition of mercury to the Great Lakes, *Environ. Res.*, 95(3), 247–265, 2004.

Patterns of mercury dispersion from emission sources

A. Kolker et al.

Title Page

Abstract

Introduction

Conclusions

References

Tables

Figures

◀

▶

◀

▶

Back

Close

Full Screen / Esc

Printer-friendly Version

Interactive Discussion



Patterns of mercury dispersion from emission sources

A. Kolker et al.

[Title Page](#)[Abstract](#)[Introduction](#)[Conclusions](#)[References](#)[Tables](#)[Figures](#)[◀](#)[▶](#)[◀](#)[▶](#)[Back](#)[Close](#)[Full Screen / Esc](#)[Printer-friendly Version](#)[Interactive Discussion](#)

Draxler, R. R. and Rolph, G. D.: HYSPLIT (HYbrid Single-Particle Lagrangian Integrated Trajectory) Model access via NOAA ARL READY Website, (<http://www.arl.noaa.gov/HYSPLIT.php>), NOAA Air Resources Laboratory, Silver Spring, MD, 2003.

Edgerton, E. S., Hartsell, B. E., and Jansen, J. J.: Mercury speciation in coal-fired power plant plumes observed at three surface sites in the southeastern US, *Environ. Sci. Technol.*, 40, 4563–4570, 2006.

Electric Energy Online: Emission control projects completed at Weston power plant, available at: http://www.electricenergyonline.com/?page=show_news&id=109588(last access: 6 January 2010), 17 April 2009.

Engle, M. A., Tate, M. T., Krabbenhoft, D. P., Kolker, A., Olson, M. L., Edgerton, E. S., DeWild, J. F., and McPherson, A. K.: Characterization and cycling of atmospheric mercury along the central US Gulf Coast, *Appl. Geochem.*, 23, 419–437, doi:10.1016/j.apgeochem.2007.12.024, 2008.

Hawthorne, M.: Big polluter to cut mercury, *Chicago Tribune*, available at:

<http://www.chicagotribune.com/news/nationworld/chi-mercury13aug13,0,7040214.story> (last access: 6 January 2010), 13 August 2007.

Hooyer, T. S.: Landscapes of Wisconsin: Madison, Wisconsin Geological and Natural History Survey, 1:500000, 2001.

Kolker, A., Engle, M. A., Krabbenhoft, D. P., and Olson, M. L.: Investigating atmospheric mercury with the USGS Mobile Mercury Laboratory, USGS Fact Sheet FS 2007-3071, 4 pp, 2007.

Kolker, A., Engle, M. A., Orem, W. H., Bunnell, J. E., Lerch, H. E., Krabbenhoft, D. P., Olson, M. L., DeWild, J. F., and McCord, J. D.: Mercury, trace elements, and organic constituents in atmospheric fine particulate matter, Shenandoah National Park, Virginia, USA: A combined approach to sampling and analysis, *Geostand. Geoanal. Res.*, 32, 279–293, 2008.

Landis, M., Stevens, R., Schaedlich, F., and Prestbo, E.: Development and characterization of an annular denuder methodology for the measurement of divalent inorganic reactive gaseous mercury in ambient air, *Environ. Sci. Technol.*, 36, 3000–3009, 2002.

Landis, M. S., Keller, G. J., Al-Wali, K. I., and Stevens, R. K.: Divalent inorganic reactive gaseous mercury emissions from a mercury cell chlor-alkali plant and its impact on near-field atmospheric dry deposition, *Atmos. Environ.*, 38, 613–622, 2004.

Patterns of mercury dispersion from emission sources

A. Kolker et al.

Title Page

Abstract

Introduction

Conclusions

References

Tables

Figures

◀

▶

◀

▶

Back

Close

Full Screen / Esc

Printer-friendly Version

Interactive Discussion

Lee, S. and Keener, T. C.: Dispersion modeling of mercury emissions from coal-fired power plants at Coshocton and Manchester, Ohio, *Ohio J. Sci.*, 108(4), 65–69, 2008.

Malcolm, E. G. and Keeler, G. J.: Evidence for a sampling artifact for particulate-phase mercury in the marine atmosphere, *Atmos. Environ.*, 41, 3352–3359, 2007.

5 Manolopoulos, H., Schauer, J. J., Purcell, M. D., Rudolph, T. M., Olson, M. L., Rodger, B., and Krabbenhoft, D. P.: Local and regional factors affecting atmospheric mercury speciation at a remote location, *J. Environ. Eng. Sci.*, 6, 491–501, 2007.

Olund, S. D., DeWild, J. F., Olson, M. L., and Tate, M. T.: Methods for the preparation and analysis of solids and suspended solids for total mercury, in: *Laboratory Analysis, Book 5, Section A, Water Analysis*, US Geological Survey, 23 pp., 2004.

10 Peltier, R.: Wisconsin Public Service Corp.'s Weston 4 earns POWER's highest honor, *Power Magazine*, 5 pp., available at: http://www.powermag.com/coal/Wisconsin-Public-Service-Corp-s-Weston-4-earns-POWERs-highest-honor_1384.html (last access: 6 January 2010), 15 August 2008.

15 Southworth, G. R., Lindberg, S. E., Zhang, H., and Anscombe, F. R.: Fugitive mercury emissions from a chlor-alkali factory: Sources and fluxes to the atmosphere, *Atmos. Environ.*, 38, 597–611, 2004.

Tewalt, S. J., Bragg, L. J., and Finkelman, R. B.: Mercury in US coal – abundance, distribution, and modes of occurrence, *US Geological Survey Fact Sheet FS-095-01*, 4 pp., 2001.

20 US Environmental Protection Agency (EPA): 2006 Toxics Release Inventory (TRI) State Data Files (Wisconsin), available at: <http://epa.gov/tri/tridata/tri06/data/index.htm#h4>, last access: 16 November 2009), 2008.

Wiener, J. G., Krabbenhoft, D. P., Heinz, G. H., and Scheuhammer, A. M.: Ecotoxicology of mercury, Chap. 16, in: *Handbook of Ecotoxicology*, 2nd edition, edited by: Hoffman, D. J., Rattner, B. A., Burton Jr., G. A., and Cairns Jr., J., CRC Press, Boca Raton, FL, USA, 407–461, 2003.

Patterns of mercury dispersion from emission sources

A. Kolker et al.

Table 1. RGM and SO₂ peak arrival time for 23 September 2007, showing simultaneous arrival of these maxima at the 50 km site and first arrival of peak RGM at the 100 km site.

23 Sep 2007	RGM		SO ₂	
	Time (GMT – 06:00)	Max. pk. ht. (pg m ⁻³)	Time (GMT – 06:00)	Max. pk. ht. (ppbv)
25 km	13:35	36.166	NA	NA
50 km	10:35	28.095*	10:30	10.41
100 km	9:35	56.783	NA	NA

* Qualified value.

Title Page

Abstract

Introduction

Conclusions

References

Tables

Figures

◀

▶

◀

▶

Back

Close

Full Screen / Esc

Printer-friendly Version

Interactive Discussion



**Patterns of mercury
dispersion from
emission sources**

A. Kolker et al.

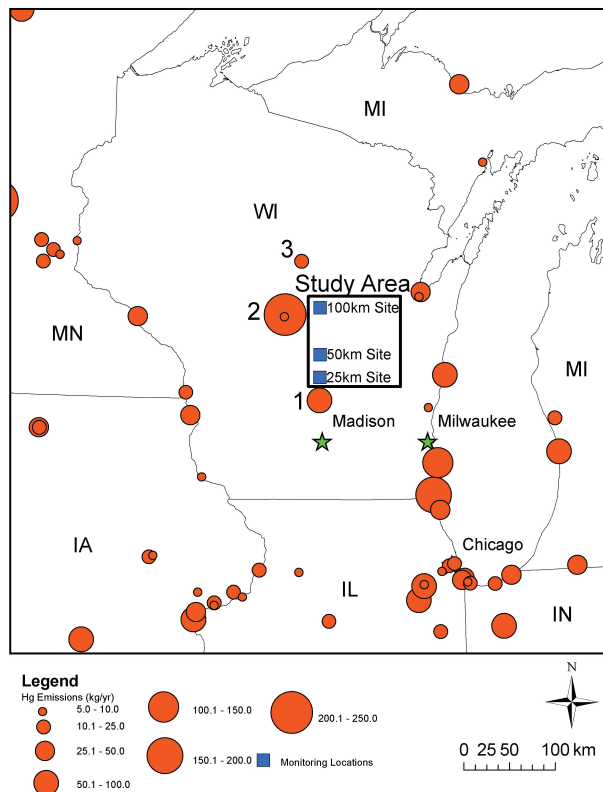


Fig. 1. Map of Wisconsin and adjoining States showing distribution of mercury emitters as of 2006, from EPA Toxics Release Inventory (EPA, 2008). Three emitters adjoin the study area: 1) 1114 MW coal-burning utility power station; 2) mercury-bed process chlor-alkali facility; 3) 465 MW coal-burning utility power station. Mercury emitters contributing 5.0 kg/yr or less are not shown.

[Title Page](#)[Abstract](#)[Introduction](#)[Conclusions](#)[References](#)[Tables](#)[Figures](#)[◀](#)[▶](#)[◀](#)[▶](#)[Back](#)[Close](#)[Full Screen / Esc](#)[Printer-friendly Version](#)[Interactive Discussion](#)

Patterns of mercury dispersion from emission sources

A. Kolker et al.

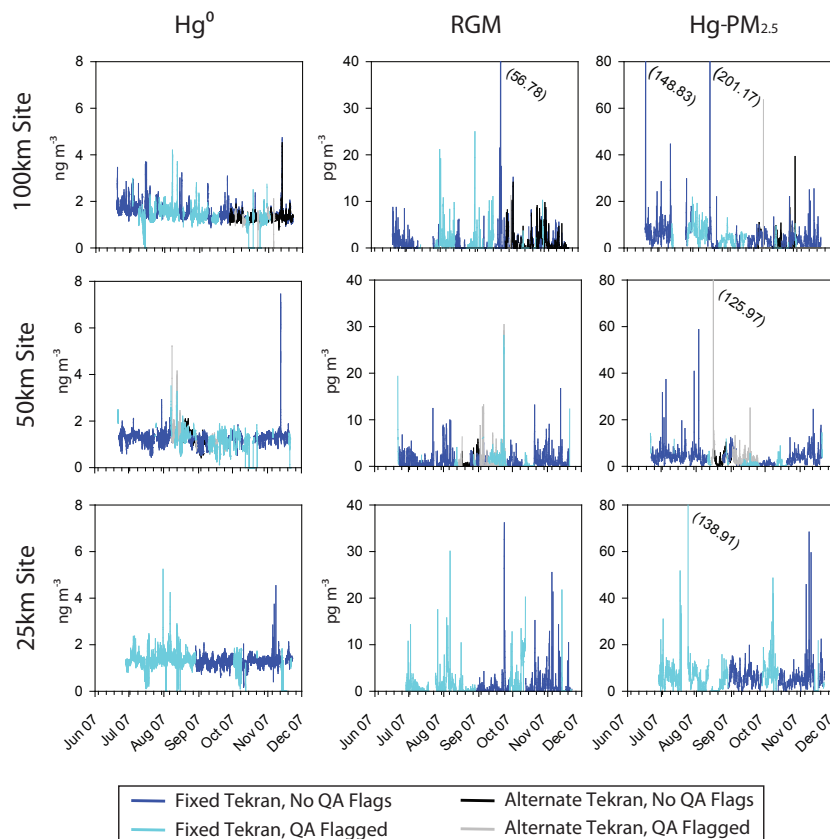


Fig. 2. Plot of cumulative mercury speciation system output for Hg° in ng m^{-3} (left), RGM in pg m^{-3} (center) and $\text{Hg-PM}_{2.5}$ in pg m^{-3} (right) for the 25 km site (bottom row), 50 km site (middle row), and 100 km site (top row). Results were collected in duplicate for the 50 km site (8 August–25 September) and the 100 km site (27 September–22 November).

Title Page

Abstract

Introduction

Conclusions

References

Tables

Figures

◀

▶

◀

▶

Back

Close

Full Screen / Esc

Printer-friendly Version

Interactive Discussion



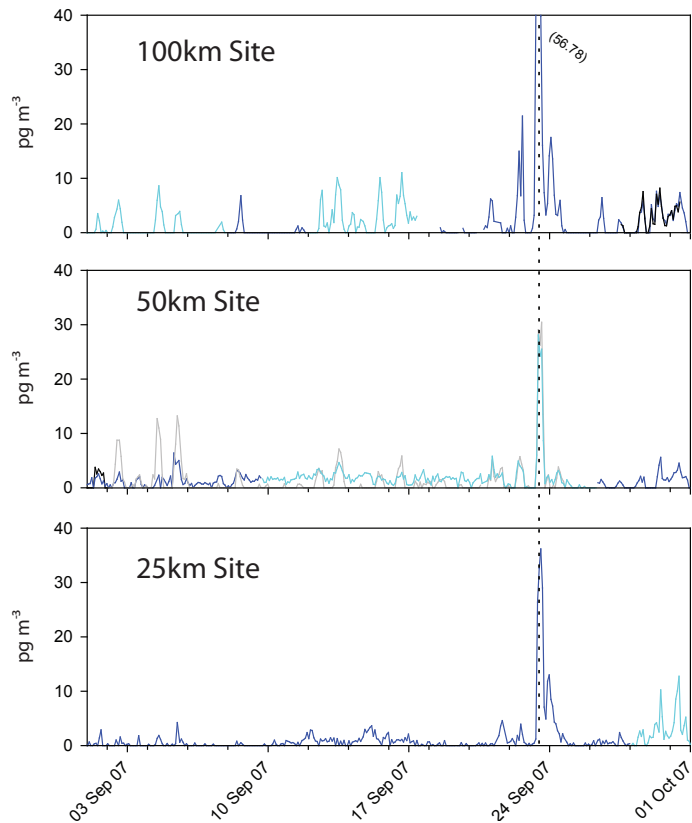


Fig. 3. Mercury speciation for September 2009 showing peak RGM exceeding 50 pg m^{-3} at the 100 km site that occurred 09:35–06:00 GMT on 23 September, and corresponding relative RGM peak heights for the 25 km site (36.17 pg m^{-3}) and the 50 km site (28.10 pg m^{-3} , qualified). The 100 km site is the farthest downwind at this time and date.

Patterns of mercury dispersion from emission sources

A. Kolker et al.

Title Page

Abstract

Introduction

Conclusions

References

Tables

Figures

◀

▶

◀

▶

Back

Close

Full Screen / Esc

Printer-friendly Version

Interactive Discussion



Patterns of mercury dispersion from emission sources

A. Kolker et al.

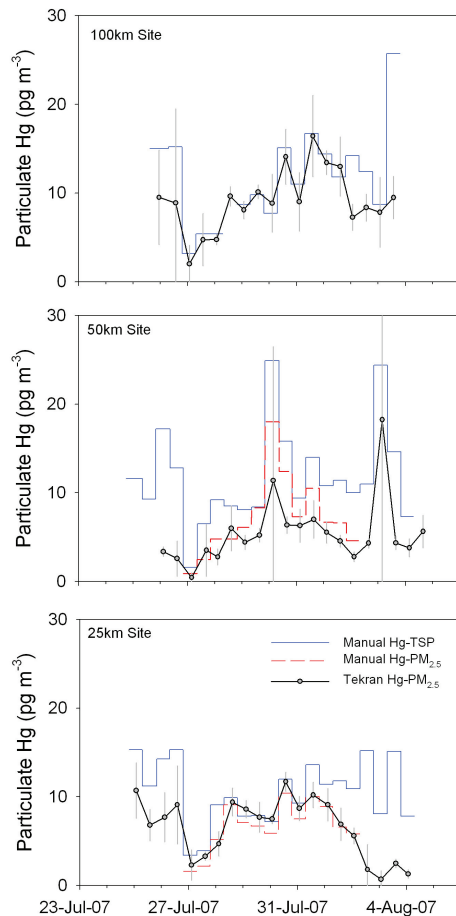


Fig. 4. Comparison of 12-h manual Hg-TSP vs. summed 12-h speciation system Hg-PM_{2.5} (25, 50, 100 km sites) and 12-h manual Hg-TSP (25, 50 km sites only), for the period of intensive Hg-PM_{2.5} sampling, 25 July–5 August 2007.

[Title Page](#)[Abstract](#)[Introduction](#)[Conclusions](#)[References](#)[Tables](#)[Figures](#)[◀](#)[▶](#)[◀](#)[▶](#)[Back](#)[Close](#)[Full Screen / Esc](#)[Printer-friendly Version](#)[Interactive Discussion](#)

Patterns of mercury dispersion from emission sources

A. Kolker et al.

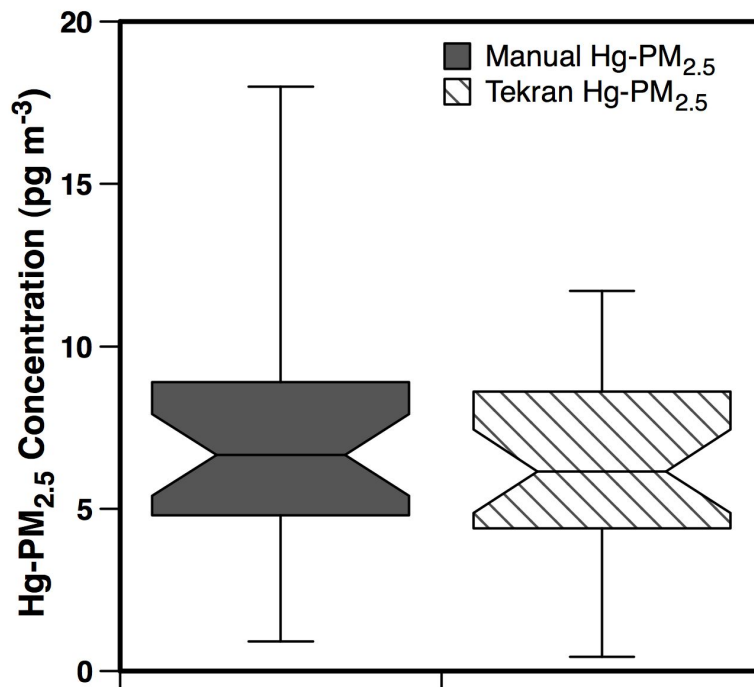


Fig. 5. Boxplot showing overlap in concentration ranges for 12-h manual Hg-PM_{2.5} vs. summed 12-h speciation system Hg-PM_{2.5} sampling, 25 July–5 August 2007.

[Title Page](#)[Abstract](#)[Introduction](#)[Conclusions](#)[References](#)[Tables](#)[Figures](#)[◀](#)[▶](#)[◀](#)[▶](#)[Back](#)[Close](#)[Full Screen / Esc](#)[Printer-friendly Version](#)[Interactive Discussion](#)

**Patterns of mercury
dispersion from
emission sources**

A. Kolker et al.

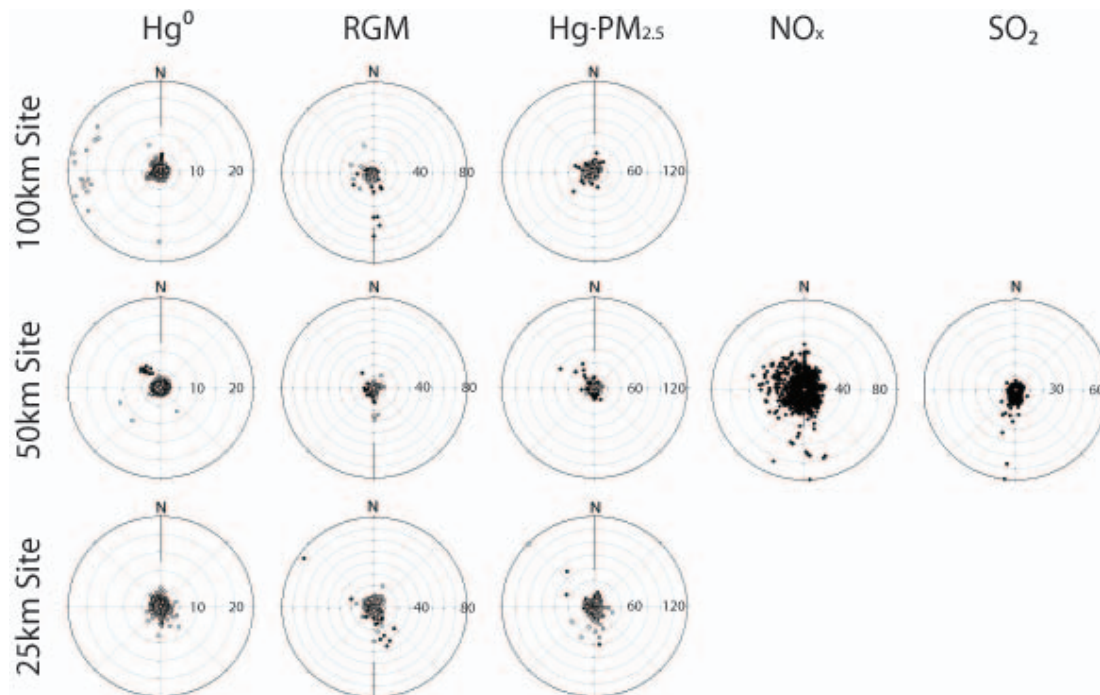


Fig. 6. Rose diagrams for mercury species (25, 50, 100 km sites) and ancillary gases (50 km site).

[Title Page](#)[Abstract](#)[Introduction](#)[Conclusions](#)[References](#)[Tables](#)[Figures](#)[◀](#)[▶](#)[◀](#)[▶](#)[Back](#)[Close](#)[Full Screen / Esc](#)[Printer-friendly Version](#)[Interactive Discussion](#)

Patterns of mercury dispersion from emission sources

A. Kolker et al.

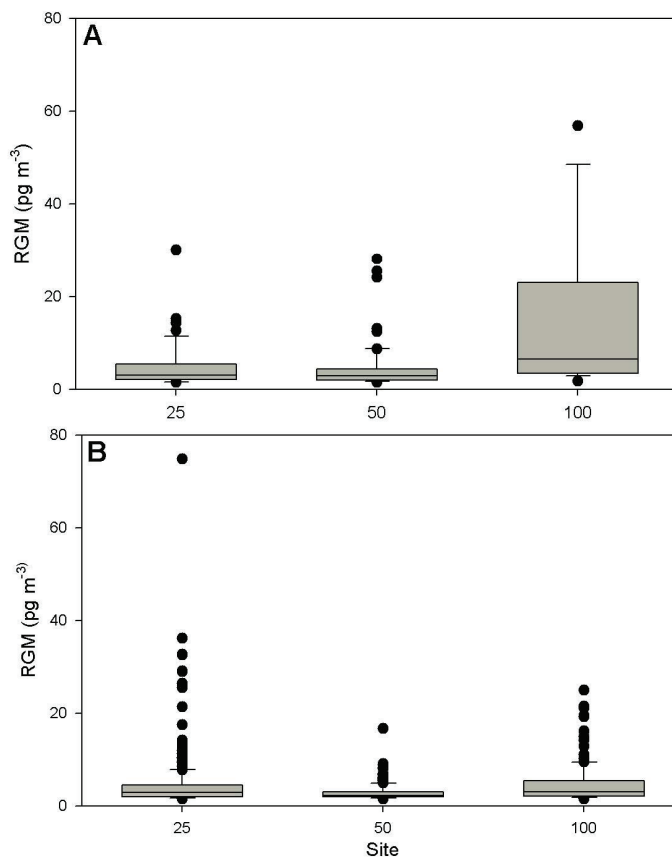


Fig. 7. Boxplots showing RGM results ($\geq 1.5 \text{ pg m}^{-3}$) for each site when winds are from the south (170–190; top panel **A**) and from all other directions (190–170; bottom panel **B**). Results do not show a consistent decrease in RGM concentration with distance from the large emission source due south of the 25 km site.

[Title Page](#)[Abstract](#)[Introduction](#)[Conclusions](#)[References](#)[Tables](#)[Figures](#)[◀](#)[▶](#)[◀](#)[▶](#)[Back](#)[Close](#)[Full Screen / Esc](#)[Printer-friendly Version](#)[Interactive Discussion](#)

Patterns of mercury dispersion from emission sources

A. Kolker et al.

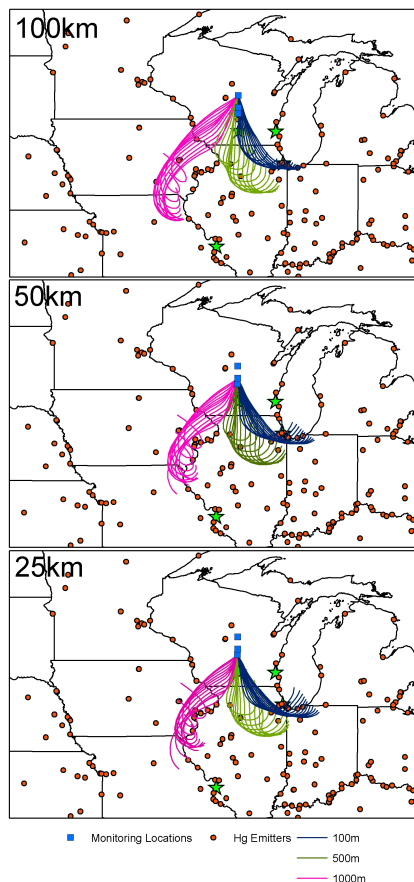


Fig. 8. NOAA HYSPLIT multiple 24-h air mass back trajectory model results for 23 September 2007. 24-h back trajectories begin each hour from 9:00 to 15:00 LT, the period of elevated RGM at each station. Results show variation in source area as a function of air mass height. This plot suggests that multiple source areas contribute to each Hg event observed.

[Title Page](#)[Abstract](#)[Introduction](#)[Conclusions](#)[References](#)[Tables](#)[Figures](#)[◀](#)[▶](#)[◀](#)[▶](#)[Back](#)[Close](#)[Full Screen / Esc](#)[Printer-friendly Version](#)[Interactive Discussion](#)